High-Temperature Adsorption of Alkali Vapors on Solid Sorbents

Vapors of alkali metal compounds can be removed from coal combustion and gasification flue gases using high-temperature aluminosilicate sorbents. The fundamentals of alkali adsorption on kaolinite, bauxite, and emathlite are compared and analyzed both experimentally and through theoretical modeling. The results show that the process is not a simple physical condensation, but a complex combination of diffusion and reaction. The kinetics of adsorption on these sorbents have similarities: the process is diffusion-influenced, the rate decreases with time, and there is a final saturation limit. There are, however, differences in reaction mechanisms leading to potentially different applications for each sorbent. In adsorbing alkali chloride vapors, kaolinite and emathlite release all the chlorine back to the gas phase while bauxite retains some of the chlorine. Moreover, the products of reaction with emathlite have a melting point significantly lower than those for kaolinite and bauxite. Therefore, emathlite is more suitable for lower-temperature sorption systems downstream of the combustors/gasifiers, while kaolinite and bauxite are suitable as *in-situ* additives.

W. A. Punjak
M. Uberoi
F. Shadman
Department of Chemical Engineering
University of Arizona
Tucson, AZ 85721

Introduction

Coal usually contains sodium and potassium minerals in various chemical and physical forms. During the combustion or gasification of coal, most of these alkali compounds are released into the gas phase and are usually present in the form of chlorides and sulfates. The vaporized alkali later condenses on various parts of the reactor and are a major cause of fouling (Borio and Levasseur, 1986). One example is the alkali-induced corrosion in combined cycle processes where the hot flue gases come in contact with ceramic turbine materials. In such applications, the alkali concentration should be reduced to less than 50 ppb to prevent significant hot corrosion.

Cleaning of coal removes some of the alkali but is not effective enough to decrease the alkali concentration to acceptable levels. A promising technique for the removal of alkali from hot flue gases is by using materials that will remove alkali vapor by adsorption and/or reaction. In general, the sorbents can be used in two ways. One method is by passing the alkali-laden flue gas through a fixed bed of an appropriate sorbent. This process has been considered for alkali removal from flue gases in the combined-cycle power generation from coal (Bachovchin et al., 1986; Jain and Young, 1985; Lee and Johnson, 1980). The second method is the injection of sorbents with coal for the in-situ capturing of alkali during pulverized coal combustion. This method has received much less attention (Shadman et al., 1987).

The choice of a suitable sorbent depends on the coal properties and the process operating conditions. In general, however, the important characteristics desired in a potential sorbent are as follows:

- High temperature compatibility
- Rapid rate of adsorption
- High loading capacity
- Transformation of alkali into a less corrosive form
- Irreversible adsorption to prevent the release of adsorbed alkali during process fluctuations

Although the use of solid sorbents for alkali and trace metal removal from flue gases has generated a lot of interest, the mechanism and the fundamental kinetics of the adsorption process are not well understood. Lee and Johnson (1980) studied the adsorption of NaCl, KCl and K_2SO_4 on a number of substrates including bauxite, silica and diatomaceous earth. They proposed chemical fixation on silica and physical adsorption on bauxite. They also found activated bauxite to be a very efficient sorbent. In another study, Lee et al. (1985) reported that the

Correspondence concerning this paper should be addressed to F. Shadman.
The current address of W. Punjak is Los Alamos National Laboratory, Los Alamos NM 87545.

adsorption of alkali on activated bauxite was by physical adsorption and chemical fixation, the latter being dominant in the presence of sufficient water vapor. Luthra and LeBlanc (1984) measured the extent of adsorption of KCl and NaCl on bauxite under different temperatures and oxygen concentrations. Their results indicated nonpreferential and reversible physical adsorption of both compounds on alumina and activated bauxite. Bachovchin et al. (1986) compared a number of additives and found that emathlite was a suitable sorbent at temperatures below 900°C.

In an earlier study in our laboratory, the kinetics and mechanism of NaCl adsorption on kaolinite was investigated (Punjak and Shadman, 1988). The results showed that kaolinite is a very effective sorbent; however, the kinetics and the mechanism of adsorption were found to depend on the gaseous atmosphere. In a typical flue gas atmosphere, the process is a combination of adsorption and chemical reaction influenced by the intraphase transport of alkali inside the porous kaolinite.

The purpose of this study is to obtain fundamental information on the kinetics and the mechanism of alkali adsorption on kaolinite, bauxite and emathlite. The kinetics of the alkali sorption process was studied at 800°C with alkali vapor concentrations of 50 to 230 ppmv in a microgravimetric reactor system. The results indicate that the sorption process is not just physical sorption, but rather a combination of adsorption and chemical reaction influenced by mass transport resistances. Both the kinetics and the mechanism depend on the physical and chemical properties of the sorbent. A theoretical model is presented that allows the extraction of intrinsic kinetic parameters from the observed data and can be used for parametric studies.

Experimental Approach

Kaolinite, bauxite and emathlite, the compositions of which are given in Table 1, were used as alkali sorbents in this study. These sorbents were used in the form of thin disks (flakes) with the approximate thickness of 0.5 mm. The flakes were devolatilized and then stored under vacuum until used.

A schematic of the experimental apparatus is shown in Figure 1. The main components of this system are an electronic microbalance (Cahn Instruments, Inc., Model 2000), a quartz reactor with inlets and outlets to maintain a controlled gas composition, a movable furnace and analyzers for determining the composition of gaseous products. The microbalance was used to monitor sorbent weight during the course of an experiment.

All experiments were performed at an adsorbent temperature

Table 1. Composition of As-received Sorbents*

	Bauxite** (wt. %)	Kaolinite† (wt. %)	Emathlite‡ (wt. %)
SiO_2	11.0	52.1	73.4
Al_2O_3	84.2	44.9	13.9
Fe_2O_3	4.8	0.8	3.4
TiO_2	—	2.2	0.4
CaO	—	—	5.0
MgO	—	—	2.6
K_2O	—	—	1.2
Na_2O	—	—	0.1

*Volatile-free basis.
**Paranam bauxite from Alcoa Corporation.
†Burgess Pigment Company.
‡Mid-Florida Mining Company.

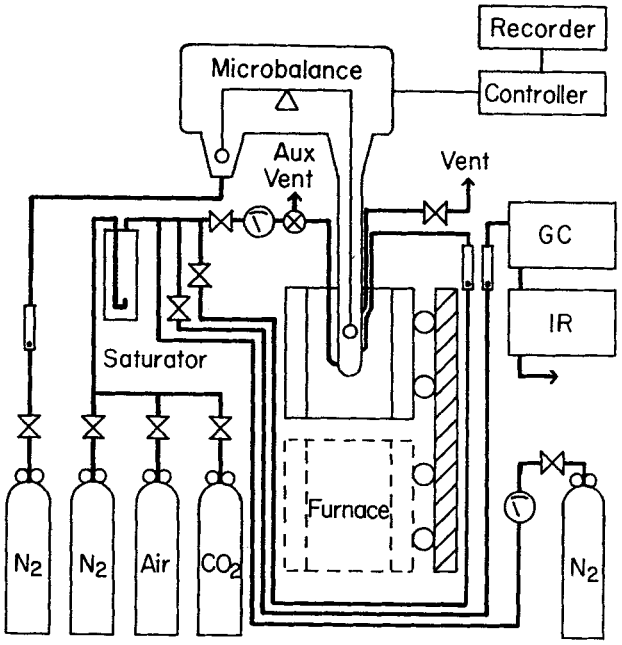

Figure 1. The apparatus.
GC = gas chromatograph; *IR* = nondispersive infrared analyzer

of 800°C using NaCl as the alkali source. A simulated flue gas (SFG) containing 80% N_2, 15% CO_2, 3% O_2 and 2% H_2O was prepared and used as a carrier for the alkali. SFG flow rates were 150 to 200 std. cm^3/min and the alkali concentrations were 50 to 230 ppmv.

Sorbent flakes were suspended from the microbalance directly above the alkali source which was placed in the bottom of the quartz reactor. The SFG was passed over the alkali source to vaporize and transport it toward the sorbent. A second SFG line, split from the first, entered the reactor a few cm above the first one and was used to dilute the alkali vapor to a desired concentration. A few cm above the sorbent the gases mixed with purging nitrogen coming down from the microbalance and went out an exhaust port. Thermocouples were placed on the outside of the reactor near the alkali source and the sorbent to monitor the temperature of each. To ensure that the SFG was not saturated with NaCl, the alkali source was always kept 10°C cooler than the sorbent. Under these conditions, there was no physical condensation of alkali on the outer surface of the particles.

The alkali vapor concentration in the gas was determined from a separate set of calibration experiments. In these experiments, the normal exhaust port was closed and the alkali-containing gas was diverted entirely into a quartz tube where all the alkali was condensed on the inner surface of the tube. After a measured period of time, the experiment was terminated and the condensed alkali was dissolved in hydrofluoric acid and measured by atomic emission spectrometry. The concentration of alkali in the gas was determined from the total alkali condensed, the flow rate and the condensation time. This calibration procedure was repeated for various flow rates and experimental conditions of interest.

An experiment was started by first closing off the normal exhaust and allowing the purge stream to flow downward over the sorbent and alkali source and then out the auxiliary vent (see Figure 1). The furnace was then raised and time allowed for the temperature and sorbent weight to stabilize. To initiate adsorp-

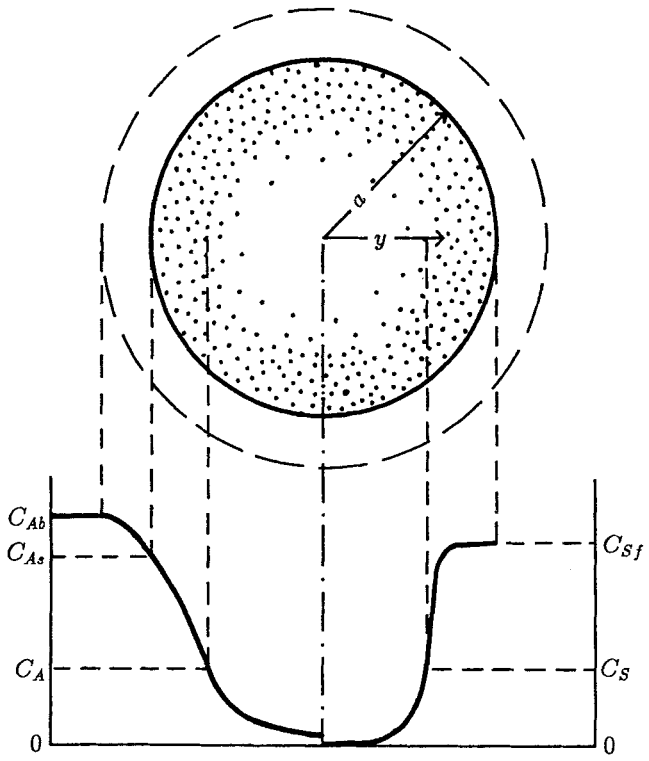

Figure 2. Partially converted sorbent particle.

tion, the normal exhaust was opened and the auxiliary exhaust was closed. At the end of the run, the flow was again reversed to stop the alkali adsorption and the furnace was lowered. In several runs, desorption of alkali was tested at the end of an adsorption cycle. To initiate desorption, the flow was reversed allowing alkali-free gas to pass over the sorbent. Desorption experiments were terminated by lowering the furnace.

Several techniques were used for chemical analysis and characterization of the samples. The bulk concentration of alkali in the sorbents was measured by atomic emission spectrometry. For these analyses, the samples were dissolved in a mixture of $H_2O/HF/HCl/HNO_3$ (5/3/1/1 proportions). The solution was then diluted by a factor of 5 with deionized water. To suppress ionization in the flame, cesium nitrate was added to provide 1000 ppm of cesium in the final solution. X-ray diffraction was

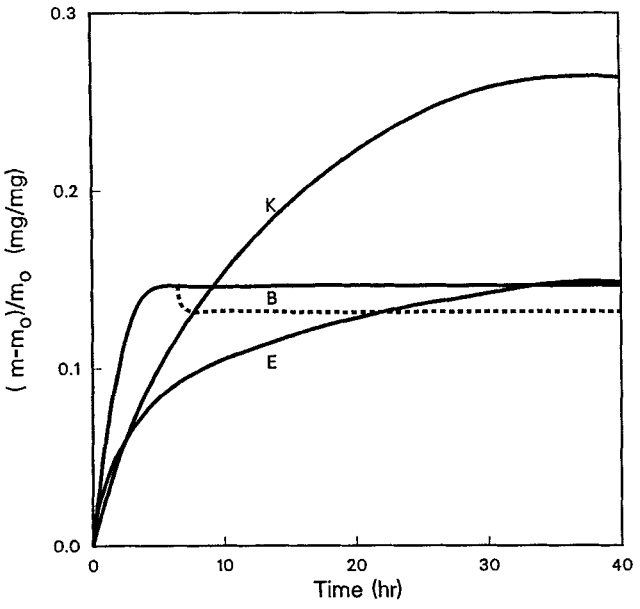

Figure 3. Temporal profile of NaCl adsorption on sorbents.

K = kaolinite, 230 ppmv Na; *B* = bauxite, 185 ppmv Na; *E* = emathlite, 150 ppmv Na

—— adsorption; – – – – desorption

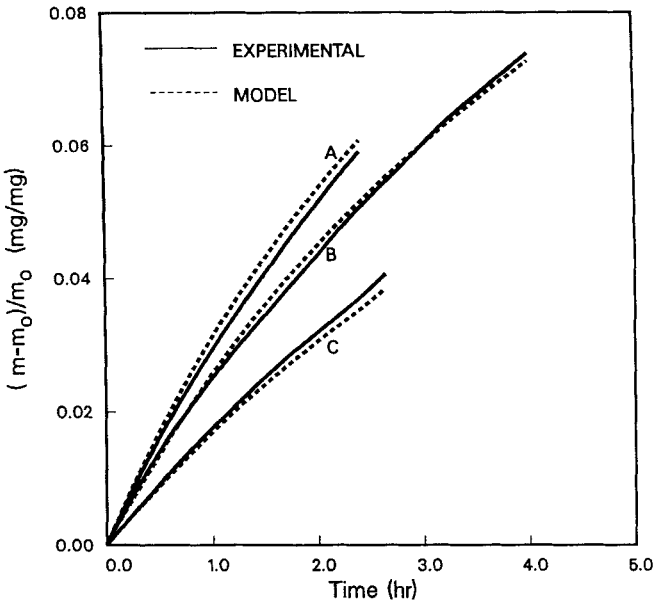

Figure 4. Temporal profile of NaCl adsorption on kaolinite.

C_{Ab} is 230 ppmv for *A*, 185 ppmv for *B*, and 135 ppmv for *C*.

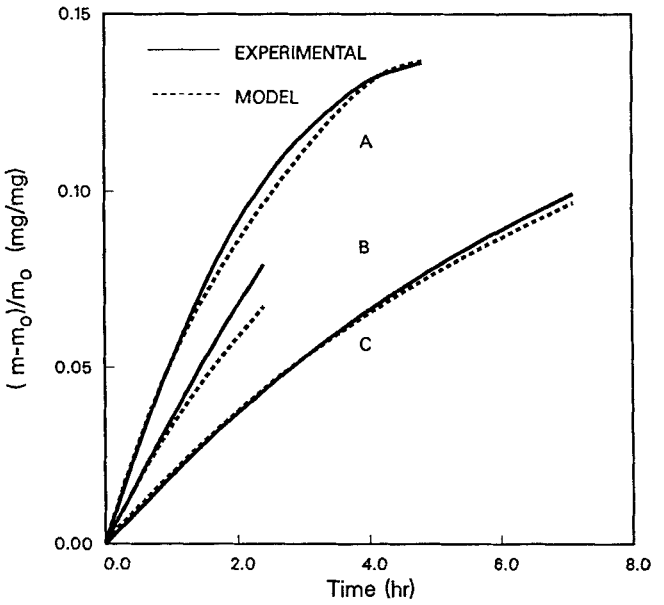

Figure 5. Temporal profile of NaCl adsorption on bauxite.

C_{Ab} is 185 ppmv for *A*, 120 ppmv for *B*, and 65 ppmv for *C*.

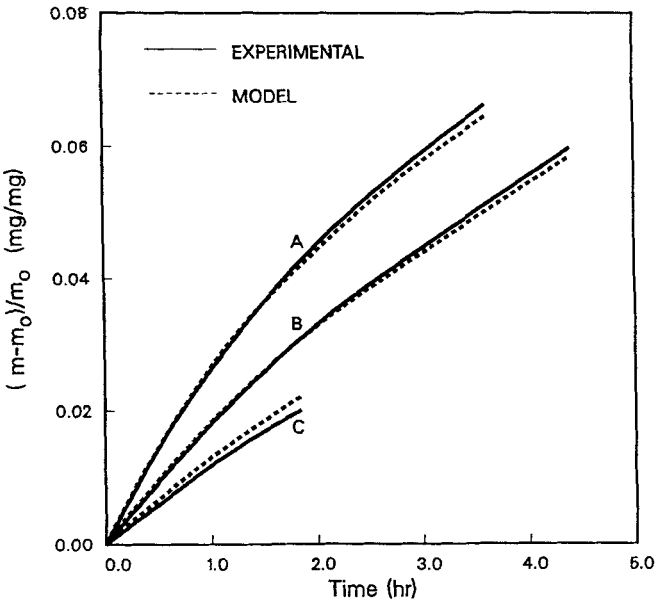

Figure 6. Temporal profile of NaCl adsorption on emathlite.

C_{Ab} is 125 ppmv for *A*, 80 ppmv for *B*, and 65 ppmv for *C*.

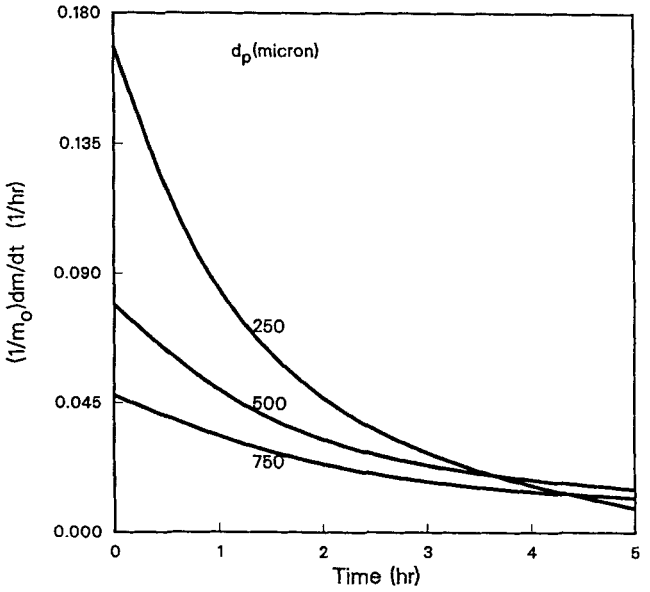

Figure 7. Effect of particle size on NaCl adsorption by kaolinite.

C_{Ab} is 200 ppmv.

used to identify crystalline phases and high-resolution scanning Auger microscopy (SAM) was used to determine the alkali distribution in the sorbents. During SAM analysis, the electron beam current was kept at 6 nA and rastered to prevent charging and damage to the samples. The porosity and pore-size distribution of the sorbents were determined by mercury porosimetry.

Theoretical Approach

A mathematical model was formulated to describe the simultaneous physical and chemical processes that occur during alkali removal by sorbent particles. Two types of geometries were considered in this study: thin flakes and spherical particles. Thin flakes represent an ideal and simple geometry which facilitates the extraction of kinetic parameters from experimental data. The spherical geometry applies to sorbent particles as used in practice. A schematic diagram of the sorbent particle and the concentration profiles are shown in Figure 2. The alkali compound, A, diffuses through the porous sorbent and is then adsorbed upon contact with the sorbent surface. The adsorption process is a combination of physical adsorption and reaction, the details of which depend on the alkali and substrate. Assuming a quasisteady state for diffusion and reaction in a porous particle, the conservation equation for alkali vapor can be written as follows:

$$\nabla \cdot D_e \nabla C_A = R_A \tag{1}$$

Table 2. Values of Model Parameters

Parameter	Bauxite	Kaolinite	Emathlite
ϵ_0	0.62	0.58	0.47
D_{eo} (cm^2/h)	260	130	190
k_m (cm/h)	5.1×10^4	5.1×10^4	5.1×10^4
C_{Sf} (gmol/cm^3 of solid)	0.017	0.023	0.019
Z	1.10	1.27	1.30
k [cm^3 of gas/(cm^3 of solid · h)]	6.1×10^7	2.1×10^7	5.9×10^7

where R_A is the molar rate of adsorption of alkali per unit bulk volume of sorbent. The boundary conditions are:

$$\nabla C_A = 0 \quad \text{at the center} \tag{2}$$

$$D_e \nabla C_A = k_m (C_{Ab} - C_A) \quad \text{at the surface} \tag{3}$$

The local alkali loading or alkali concentration in the solid phase, C_S, is given by the following conservation equation:

$$(1 - \epsilon_0) \frac{\partial C_S}{\partial t} = R_A \tag{4}$$

with the initial condition:

$$C_S = 0 \quad \text{at} \quad t = 0 \tag{5}$$

It is assumed that the local rate of adsorption is given by the following rate expression:

$$R_A = (1 - \epsilon_0)\, k C_A (1 - C_S/C_{Sf}) \tag{6}$$

The variations in the effective diffusivity are given by:

$$D_e = \frac{\epsilon^2}{\epsilon_0^2} D_{e0} \tag{7}$$

where ϵ varies during adsorption as follows:

$$\epsilon = \epsilon_0 - (Z - 1)(1 - \epsilon_0) \cdot \frac{C_S}{C_{Sf}} \tag{8}$$

Equations 1, 2 and 3 were solved numerically using a variable-step central-difference technique. Equation 4 was solved simultaneously using a fourth-order Runge-Kutta technique.

The overall alkali loading, X_T, at any time is obtained by integrating C_S over the sorbent volume:

$$X_T = \frac{1}{V_S C_{Sf}} \oint_0^{V_S} C_S \, dV \tag{9}$$

The mass gain is given by the product of X_T and α, the maximum fractional mass gain at saturation.

Discussion of Results

Typical experimental weight gain profiles for the three sorbents tested are shown in Figure 3. The results indicate a decrease in adsorption rate with loading and a final alkali saturation limit. Bauxite is observed to have the highest initial rate while kaolinite has the largest capacity. Weight gain profiles for the three sorbents at different alkali vapor concentrations are shown in Figures 4–6. As expected, an increase in the alkali concentration results in an increase in the rate.

An important difference between the adsorption characteristics of the three sorbents is the reversibility of the adsorption process. After saturation, the reversibility of the alkali uptake was tested for each sorbent following the procedure described in the experimental section. No desorption was observed for kaolinite and emathlite, but bauxite lost approximately 10% of its total weight gain. This suggests that the mechanism of adsorption is not the same for the three sorbents.

The model developed in the previous section was used to extract intrinsic kinetic information from the weight gain profiles. A list of parameters used with the model is given in Table 2. The overall rate constant, k, for each sorbent was obtained by fitting the model to the initial rate data. These rate constants together with the other parameters were then used to predict

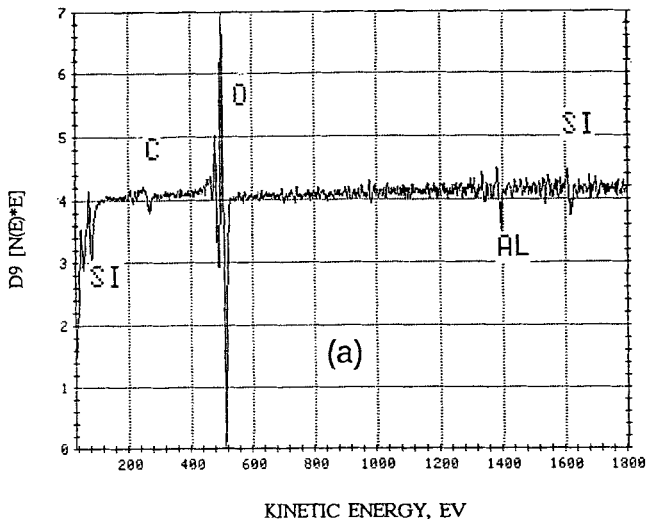

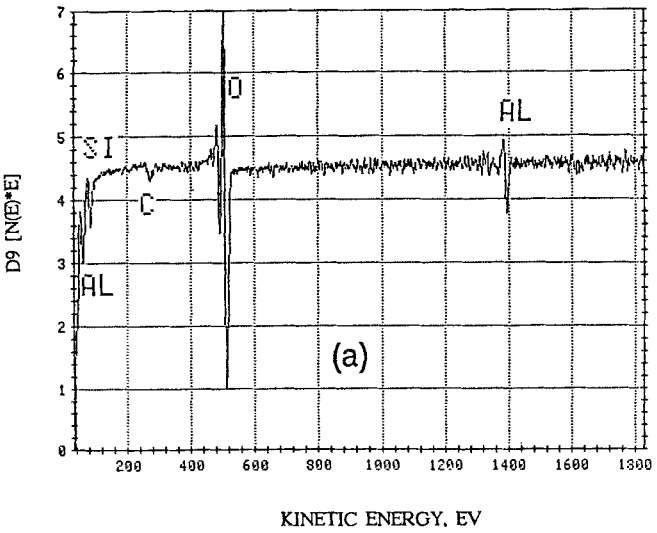

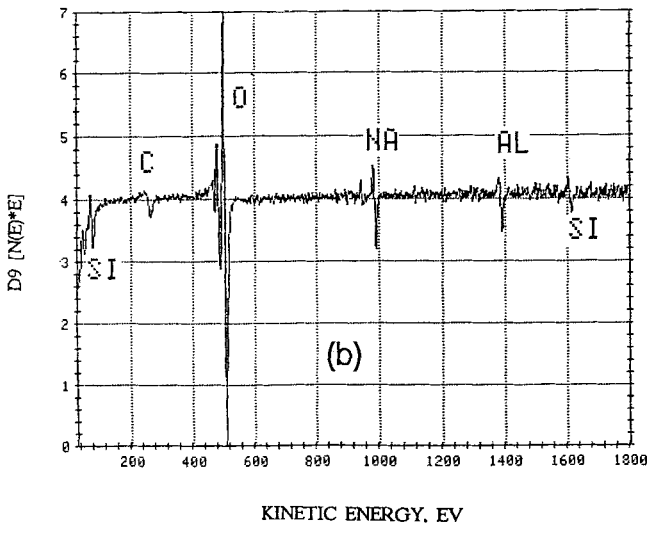

a) Before alkali adsorption;
b) after alkali adsorption

Figure 8. Auger spectra of kaolinite.

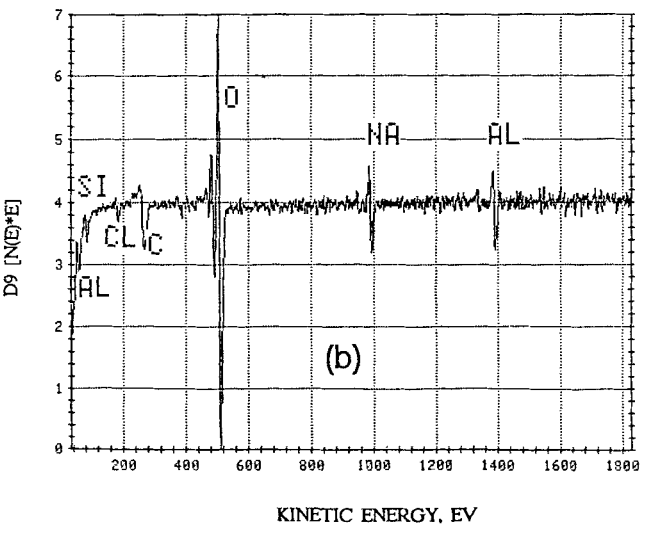

a) Before alkali adsorption;
b) after alkali adsorption

Figure 9. Auger spectra of bauxite.

weight gain profiles for the three sorbents at different alkali concentrations as shown in Figures 4–6. It can be seen that the model closely approximates the experimental data. Obviously, by the very nature of formulation, the model predictions coincide with the experimental data at full conversions.

The values of rate coefficients estimated from the model are given in Table 2. The difference in the rate coefficients shows that the adsorption process is not a physical and nonselective process but rather a chemical process which depends on the chemical nature of the sorbent. The kinetic parameters suggest that in applications where sorbent particles are larger than 80 μm, both interphase and intraphase diffusional resistances influence the observed kinetics for all three sorbents.

The proposed model is an effective tool for data extrapolation and parametric study. As an example, Figure 7 illustrates the effect of particle size on the adsorption kinetics. The results indicate that the rate of adsorption is very sensitive to particle size. In general, particle size is selected to maximize the rate of alkali removal and the additive utilization efficiency (fraction of the additive reacted). For applications in which alkali is removed inside the combustor, the residence time of the sorbent particles is usually a few seconds. In such applications the particles should be small (typically less than 200 μm) to provide rapid kinetics and high sorbent utilization. In applications where alkali removal is downstream from the combustor, a fixed bed of relatively large particles can be used. Larger particles are easier to handle and cause less attrition and particulate emission.

To gain insight into the mechanism of alkali/sorbent interactions, the fresh and fully saturated sorbents were analyzed using various chemical analytical techniques. In particular, the XRD and SAM analyses provided useful information on the nature and distribution of alkali on the sorbents. The differentiated SAM spectra for kaolinite, bauxite and emathlite are shown in Figures 8, 9 and 10, respectively. One important difference between the substrates revealed by these results is in the ratio of sodium to chlorine adsorbed. Chlorine, which has a peak at 176 eV, was not observed in the products of adsorption on emathlite

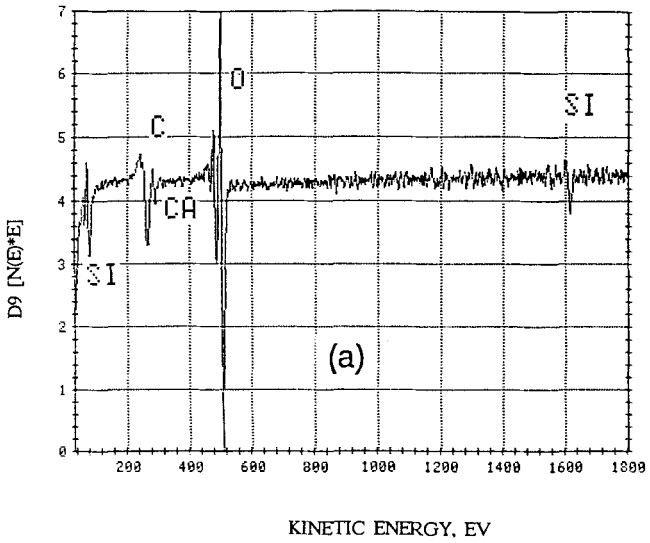

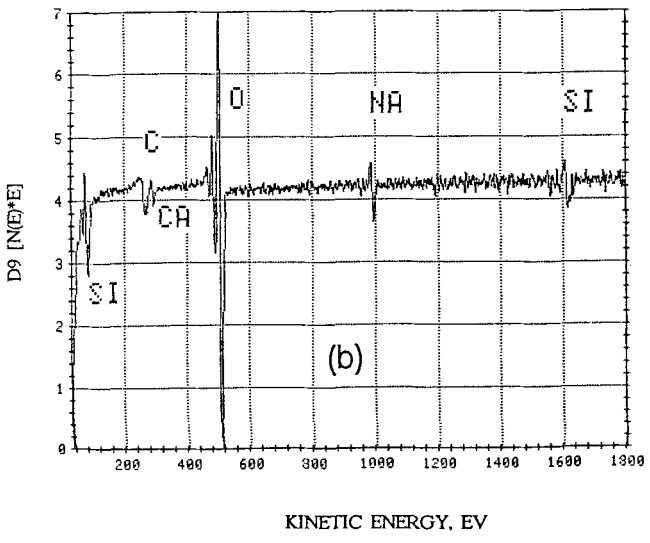

a) Before alkali adsorption;
b) after alkali adsorption

Figure 10. Auger spectra of emathlite.

(a)

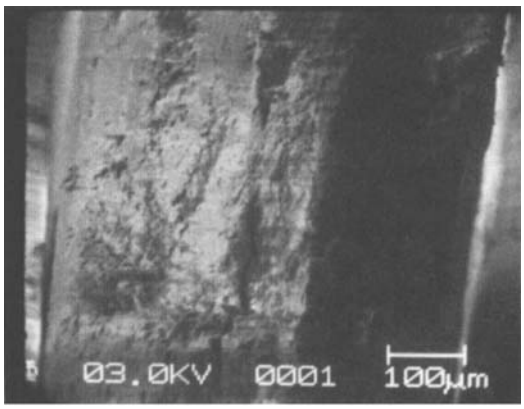

(b)

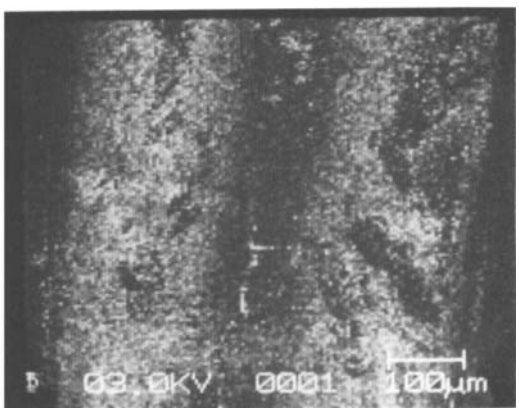

Figure 11a. Scanning electron micrograph of the cross section of a partially converted kaolinite flake.

Figure 11b. Alkali concentration map of the cross section shown in Figure 11a.

and kaolinite. In contrast, chlorine was partially retained by bauxite. This has important implications in the selection of sorbents where chlorine removal is a concern.

To study the changes in the substrate during adsorption, the cross sections of partially converted samples were examined. The progress of reaction was visible in the kaolinite samples because of the noticeable color difference between the beige, product layer and the white, unreacted core. However, similar layers were not visible in bauxite and emathlite. Alkali profiles were obtained by examining the cross sections of some partially converted flakes with scanning Auger microscopy. The SEM and SAM results for kaolinite are shown in Figure 11. The brightest regions of the map in Figure 11b are areas of highest alkali concentration. The alkali content was observed to be largest near the outer edge, decreasing rapidly toward the flake center. Alkali maps obtained for bauxite (Figure 12) and emathlite showed similar results. This indicates that the adsorption/reaction process for all three sorbents under the experimental conditions used was influenced by intraphase diffusion. This is in agreement with the model predictions.

X-ray diffraction (XRD) spectra obtained for the sorbents prior to and after alkali adsorption indicate the formation of several reaction products. As shown in Figure 13, the saturated kaolinite contains primarily nephelite and carnegieite which are sodium aluminosilicate polymorphs with the chemical formula $Na_2O \cdot Al_2O_3 \cdot 2SiO_2$. In nephelite, which is thermodynamically favored at high temperatures, the sodium cation is octahedrally coordinated whereas in carnegieite it is tetrahedrally coordinated (Falcone and Schobert, 1986). Based on this information and the absence of chlorine in the adsorption product, the following reaction scheme is proposed:

$$\underbrace{Al_2O_3 \cdot 2SiO_2}_{\text{metakaolinite}} + 2NaCl + H_2O \rightarrow \underbrace{Na_2O \cdot Al_2O_3 \cdot 2SiO_2}_{\text{nephelite/carnegieite}} + 2HCl\uparrow \quad (10)$$

where metakaolinite is the dehydration product of kaolinite. The stoichiometry of this reaction suggests a 27.9% increase in sample weight on completion conversion. This is very close to the observed 26.6%. In addition, the alkali uptake determined by atomic emission analysis is very close to what Reaction 10 predicts. Kühn and Plogmann (1983) and Falcone and Schobert (1986) also observed the formation of nephelite when a mixture of sodium compounds and kaolinite was heated to high temperatures. Due to the high melting point of nephelite (1,526°C), kaolinite would be a suitable sorbent for the *in-situ* capture of alkali at high temperatures. It is also an excellent choice for the downstream removal of alkali because of its high capacity.

Similar results for bauxite indicate a more complicated process. The XRD spectrum for as-received bauxite shows the pres-

(a)

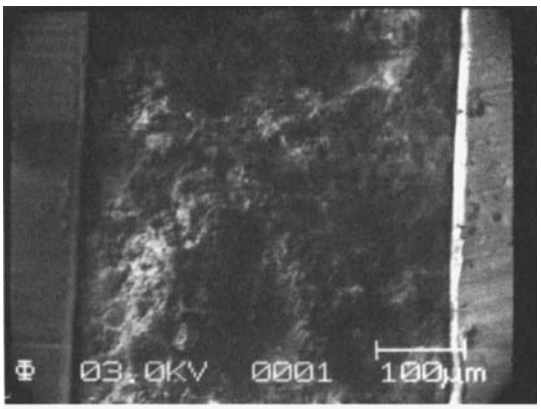

(b)

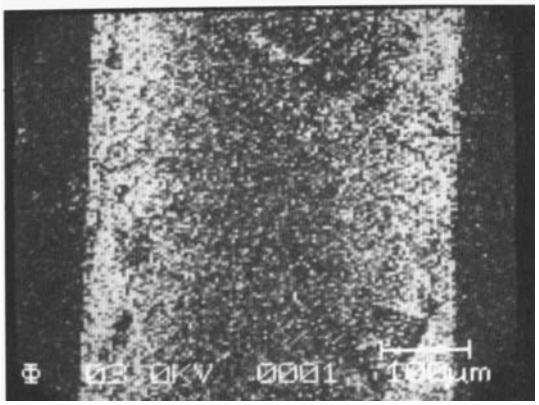

Figure 12a. Scanning electron micrograph of the cross section of a partially converted bauxite flake.

Figure 12b. Alkali concentration map of the cross section shown in Figure 12a.

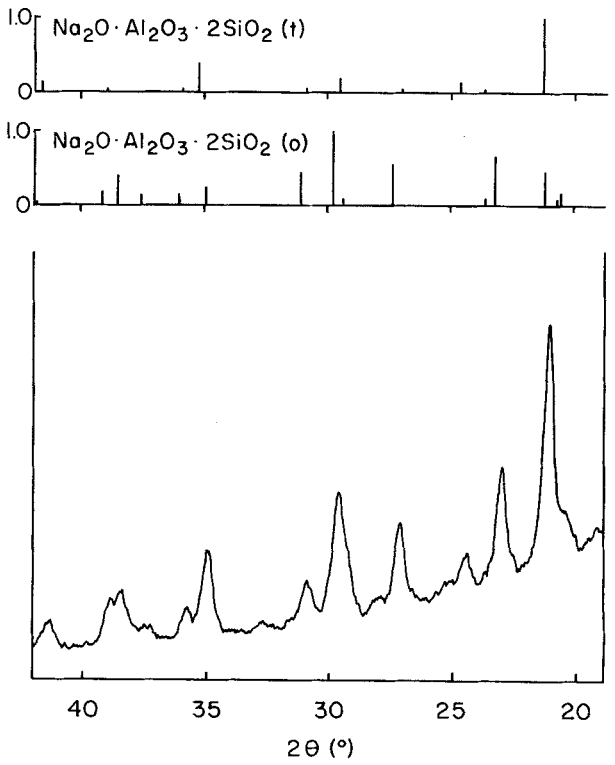

Figure 13. X-ray diffraction spectrum of fully saturated kaolinite.
t = carnegieite; o = nephelite

ence of α-quartz, corundum and hematite. The XRD results on fully saturated bauxite (Figure 14) indicate the formation of nephelite and carnegieite produced by a reaction similar to Reaction 10. However, the amount of silica in bauxite is not sufficient for Reaction 10 to account for all the adsorbed alkali. Apparently, the rest of the alkali is present as glassy products or physisorbed chloride not detectable by XRD. Since chlorine is lost from the saturated product during desorption, physisorbed NaCl might be the portion which is removed during the desorption experiments. The non-dissociative adsorption of alkali chlorides on alumina has been reported previously (Luthra and LeBlanc, 1984; Shadman and Punjak, 1986). Hematite, present both before and after adsorption, did not undergo any noticeable transformation.

The XRD results for emathlite show the presence of aluminosilicate (Al_2SiO_5), α-quartz and cristobalite before alkali adsorption. The fully saturated sample (Figure 15) consisted primarily of albite ($Na_2O \cdot Al_2O_3 \cdot 6SiO_2$) together with smaller amounts of sodium calcium aluminate ($NaCa_4Al_3O_9$). Therefore, much of the sodium capture by emathlite can be described by the following overall reaction:

$$5SiO_2 + Al_2SiO_5 + 2NaCl + H_2O \rightarrow \underbrace{Na_2O \cdot Al_2O_3 \cdot 6SiO_2}_{\text{albite}} + 2HCl\uparrow \quad (11)$$

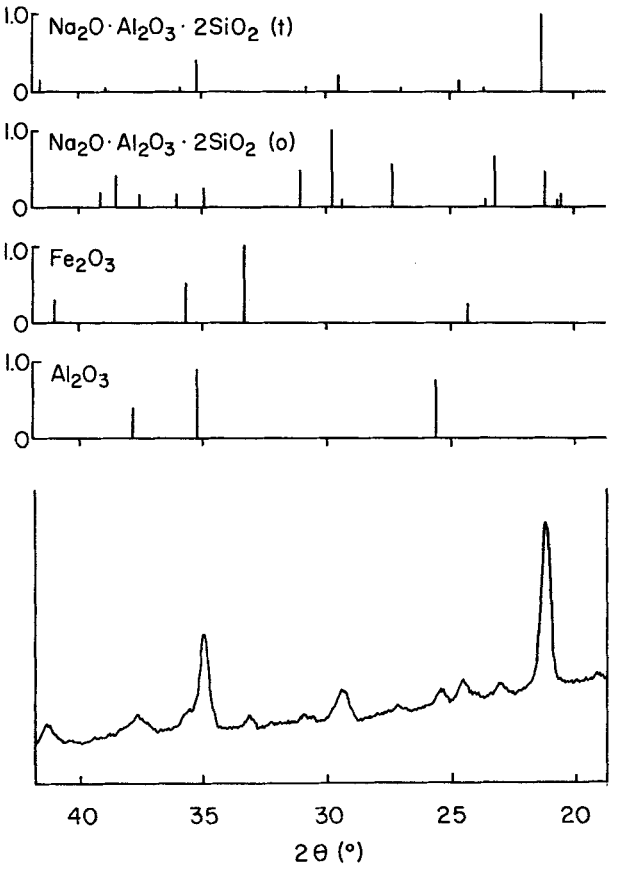

Figure 14. X-ray diffraction spectrum of fully saturated bauxite.
t = carnegieite; o = nephelite

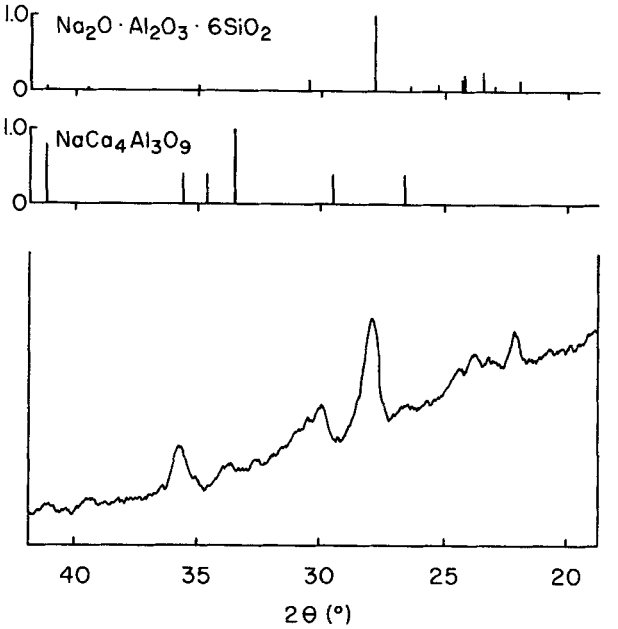

Figure 15. X-ray diffraction spectrum of fully saturated emathlite.

This agrees with the prediction of Bachovchin et al. (1986) about the formation of albite based on thermodynamic calculations.

The above results indicate important differences in the potential applications of these three sorbents. Kaolinite and emathlite have the disadvantage of releasing all the chlorine back to the gas phase; this is a disadvantage where chlorine in the gas phase is also a concern. Since some alkali is reversibly adsorbed on bauxite, process fluctuations can result in the release of this alkali back into the flue gas. A possible problem with emathlite as a sorbent is the presence of a relatively large amount of potassium in the as-received material (Table 1). Atomic emission analysis of emathlite before and after exposure to NaCl showed that the potassium content dropped from 0.89 wt. % to 0.07 wt. %. This indicates the release of a significant amount of potassium which adds to the overall alkali problem. Another important difference is in temperature compatibility. Since the melting point of albite (1,100°C) is much lower than that of nephelite (1,526°C), emathlite is more suitable for lower temperature applications such as in the downstream clean up of flue gas.

For solvent injection in pulverized coal combustors, two additional points should be considered. The first point is the possibility of alkali condensation on the outer surface of the sorbent particles. This occurs when alkali vapors become supersaturated due to rapid cooling or reactions. The present results do not include condensation and pore plugging; however, a study of alkali sorbent interactions under these conditions is in progress. The second consideration is the relatively short residence time for sorbent particles in pulverized combustors. Under these conditions the sorbent conversion is generally low but can be improved by using smaller particles.

Conclusions

• Kaolinite, bauxite and emathlite are suitable sorbents for the removal of alkali vapors from hot flue gases. However, ka-

olinite and bauxite are more suitable than emathlite at temperatures above 1,000°C (e.g., *in-situ* alkali removal).

- The rate of adsorption decreases with alkali loading and drops to zero when a final saturation limit is achieved. This saturation limit is the highest for kaolinite.
- The adsorption of alkali chloride on kaolinite and emathlite is irreversible with the release of chlorine back to the gas phase as HCl vapor. The adsorption on bauxite is partially reversible and a portion of the chlorine is retained.
- Interphase and intraphase diffusional resistances influence the kinetics of the adsorption process in the range of practical interest.
- The proposed theoretical model agrees with the experimental data and can be used for design and parametric studies.

Acknowledgment

This work was supported by the US Department of Energy, Pittsburgh Energy Technology Center (grant number DE-FG22-86PC90505). A T. G. Chapman Alumni Fellowship for W. A. Punjak and an Arizona Mining and Mineral Resources Research Institute Fellowship for M. Uberoi are also gratefully acknowledged.

Notation

a = particle radius, cm
C_A = concentration of alkali, gmol/cm^3 of gas
C_{Ab} = concentration of alkali in bulk gas, gmol/cm^3 of gas
C_S = alkali loading, gmol of adsorbed alkali/cm^3 of solid sorbent
C_{Sf} = the maximum value of C_S at saturation
d_p = particle diameter, μm
D_e = effective diffusivity of alkali in sorbent, cm^2/h
D_{e0} = initial effective diffusivity of alkali in sorbent, cm^2/h
k = rate coefficient, cm^3 of gas/cm^3 of solid sorbent · h
k_m = interphase mass-transfer coefficient, cm/h
m = mass of the sorbent at time t, g
m_0 = initial mass of the sorbent, g
m_f = final mass of the sorbent at saturation, g
R_A = local rate of adsorption, gmol/cm^3 of bulk sorbent · h
t = time, h
V_S = volume of sorbent, cm^3
X_T = overall fractional loading of sorbent
y = distance from the center of the slab or sphere, cm
Z = ratio of skeletal volume of saturated sorbent to skeletal volume of initial sorbent

Greek letters

$\alpha = (m_f - m_0)/m_0$
ϵ = porosity of the sorbent
ϵ_0 = initial porosity of the sorbent

Literature Cited

Bachovchin, D. M., M. A. Alvin, E. A. DeZubay, and P. R. Mulik, "A Study of High Temperature Removal of Alkali in a Pressurized Gasification System," DOE-MC-20050-2226, Westinghouse Res. Dev. Center, Pittsburgh (1986).

Borio, R. W., and A. A. Levasseur, "Coal Ash Deposition in Boilers," in "Mineral Matter and Ash in Coal," K. S. Vorres, ed.; *ACS Symp. Ser.*, 301; Ch. 21 (1986).

Falcone, S. K., and H. H. Schobert, "Mineral Transformations During Ashing of Selected Low Rank Coals," *Mineral Matter and Ash in Coal*, K. S. Vorres, ed., *ACS Symp. Ser.*, 301, Ch. 9 (1986).

Jain, R. C., and S. C. Young, "Laboratory/Bench Scale Testing and Evaluation of A.P.T. Dry Plate Scrubber," DOE-ET-15492-2030, Air Pollution Technology, Inc., San Diego (1985).

Kühn, L., and H. Plogmann, "Reaction of Catalysts with Mineral Matter during Coal Gasification," *Fuel*, **62**, 205 (1983).

Lee, S. H. D., and I. Johnson, "Removal of Gaseous Alkali Metal Compounds from Hot Flue Gas by Particulate Sorbents," *J. Eng. Power*, **102**, 397 (1980).

Lee, S. H. D., R. F. Henry, and K. M. Myles, "Removal of Alkali Vapors by a Fixed Granular-Bed Sorber Using Activated Bauxite as a Sorbent," CON-8503513, Argonne National Lab, Argonne, IL (1985).

Luthra, K. L., and O. H. LeBlanc, "Adsorption of NaCl and KCl on Al_2O_3 at 800–900°C," *J. Phys. Chem.*, **88**, 1896 (1984).

Punjak, W. A., and F. Shadman, "Aluminosilicate Sorbents for Control of Alkali Vapors During Coal Combustion and Gasification," *Energy and Fuels*, **2**, 702 (1988).

Shadman, F., T. W. Peterson, J. O. L. Wendt, W. A. Punjak, and R. G. Rizeq, "Mechanism of Surface Enrichment and Adhesion of Coal Combustion Particulates," 2nd quarterly report, DE-FG22-86PC90505, U.S. Dept. of Energy (PETC) (1987).

Shadman, F., and W. A. Punjak, "Solid Adsorbents for the Control of Alkali in Combustion Systems," Combustion Inst., Tucson (1986).

Manuscript received Aug. 22, 1988, and revision received Mar. 13, 1989.